THE JOURNAL OF PHYSICAL CHEMISTRY C

Article

Cite This: J. Phys. Chem. C 2018, 122, 9499−9506

pubs.acs.org/JPCC

# Real-Time in Situ Investigation of Supramolecular Shape Memory Process by Fluorescence Switching

Wei Lu,[†] Chunxin Ma,[†] Dong Zhang,[‡] Xiaoxia Le,[†] Jiawei Zhang,*[,†] Youju Huang,[†] Chih-Feng Huang,[§] and Tao Chen*[,†,∥]

[†]Key Laboratory of Marine Materials and Related Technologies, Zhejiang Key Laboratory of Marine Materials and Protective Technologies, Ningbo Institute of Materials Technology and Engineering, Chinese Academy of Sciences, Ningbo 315201, China

[‡]College of Materials Science & Engineering, Zhejiang University of Technology, Hangzhou 310014, China

[§]Department of Chemical Engineering, National Chung Hsing University, Taichung 402, Taiwan

[∥]University of Chinese Academy of Sciences, 19A Yuquan Road, Beijing 100049, China

Supporting Information

**ABSTRACT:** Shape memory hydrogels (SMHs) that take advantage of supramolecular chemistry cross-links to fix temporary shapes at room temperature are newly developed important shape memory polymers. It is thus highly desirable to explore in detail the in situ formation and real-time spatial distribution of temporary supramolecular cross-links in SMH systems, which can provide more in-depth information about the shape memory mechanism and promote the fabrication of new SMHs. However, related study still remains very challenging. We herein report the development of a special SMH system that involves fluorescent alginate−$Eu^{3+}$ complexes as switching cross-links. Its coordination-triggered supramolecular shape memory/recovery processes and dynamics could be directly visualized by a high-contrast fluorescence imaging method. Remarkably, this efficient and sensitive fluorescence study enables real-time in situ monitoring of the process, in which $Eu^{3+}$ ions gradually diffuse into the hydrogel sample and chelate with alginate to form the $Eu^{3+}$−Alg temporary cross-links. Furthermore, a theoretical model correlating the fluorescence intensities of the SMH system with their shape memory effect (SME) was successfully established, which allows the facile and accurate prediction of both the shape memory and recovery ratios on the basis of quantitative emission spectral results. These details disclosed in this study will thus deepen the understanding of supramolecular shape memory process and mechanisms and accelerate the development of new practical shape memory hydrogels in the future.

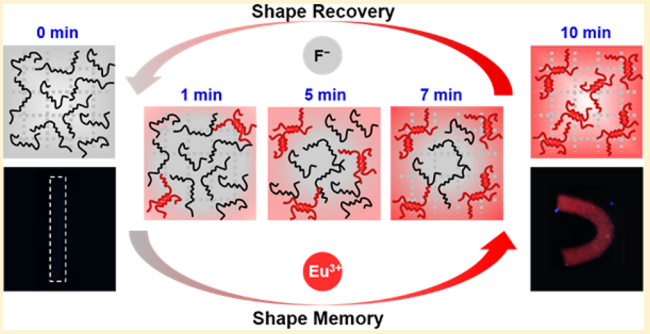


## 1. INTRODUCTION

As an important type of shape memory polymers (SMPs),[1−18] shape memory hydrogels (SMHs),[19] which take advantage of reversible cross-links (e.g., supramolecular interactions and dynamic covalent bonds) to fix temporary shapes at room temperature, are attracting increasing research attention these days. During the past few years, a large number of advanced and elegant SMHs have been successfully constructed by us[20−22] and other research groups,[23−38] which have presented many potential applications in the fields of smart textiles, soft robotics, biomedicine, etc. Due to the highly reversible nature of supramolecular chemistry,[39−41] SMHs can exhibit excellent cycled shape memory behavior at room temperature through dynamic dissociation and recombination of the reversible cross-links. In other words, supramolecular shape memory is a dynamic process that is determined and regulated by the temporary supramolecular cross-links. Direct investigation of in situ formation and real-time spatial distribution of supramolecular temporary cross-links in SMH systems will give us more in-depth information about the mechanism of shape memory process, thus significantly promoting the design and preparation of highly desirable SMHs. However, detailed exploration of such molecular-level supramolecular chemistry process and dynamics in SMHs still remains a great challenge.

Customarily, the study of supramolecular shape memory process is performed by the bending test, in which a straight hydrogel sample is first bent at a given angle under external forces and then fixed via the temporary cross-links.[1,20] After release of the deforming stress, the bending angle of the temporary shape is determined. This method is easy to implement and can be used to roughly assess the shape memory effect (SME) of hydrogel samples, but it fails to provide any information on in situ formation and real-time distribution of temporary supramolecular switches. Usually, the

Received: February 18, 2018
Revised: April 9, 2018
Published: April 16, 2018







DOI: 10.1021/acs.jpcc.8b01689
J. Phys. Chem. C 2018, 122, 9499−9506

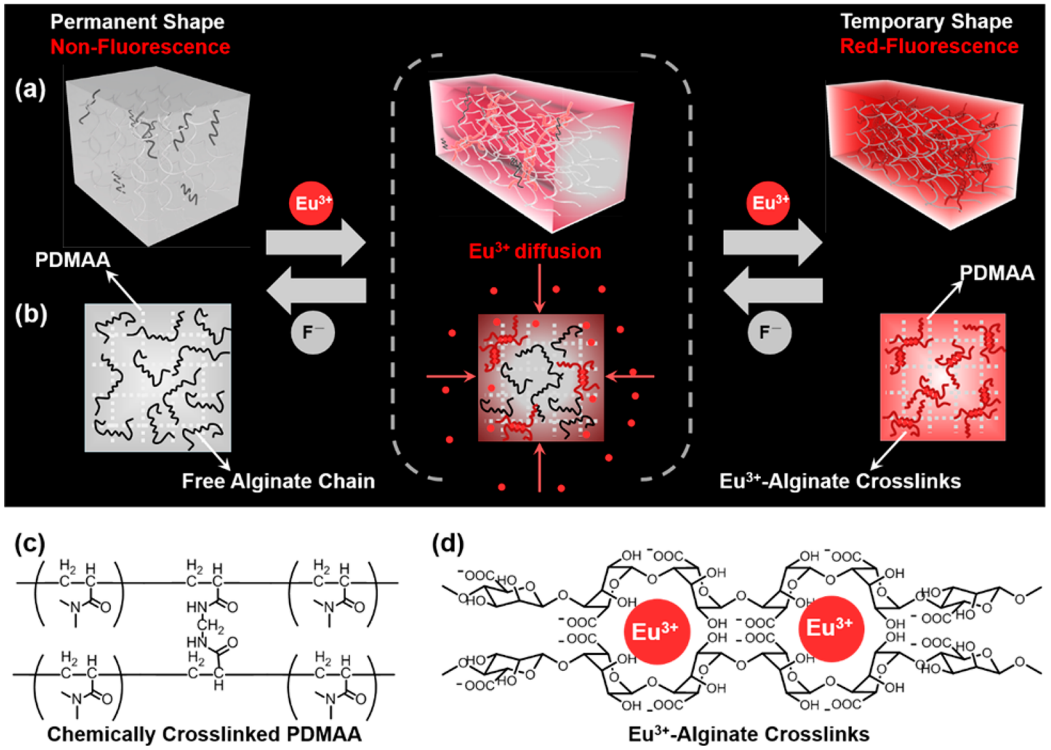


**Figure 1.** Illustration showing the $Eu^{3+}$-triggered shape memory process of PDMAA−Alg hydrogels: (a) general and (b) cross-sectional views, as well as (c, d) chemical structure of the hydrogel. PDMAA−Alg hydrogels were prepared by thermally induced radical polymerization of DMAA monomer and *N,N′*-methylenebis(acrylamide) cross-linker in the presence of sodium alginate. The developed hydrogel system employs the chemically cross-linked PDMAA network and $Eu^{3+}$ cross-linked Alg network as the permanent and temporary cross-links, respectively. Since the Alg−$Eu^{3+}$ complexes are known to emit vivid red light, the dynamic metal coordination-triggered supramolecular shape memory process could be visualized directly and quantitatively studied by fluorescence imaging method. Importantly, in situ formation and real-time distribution of supramolecular temporary ($Eu^{3+}$−Alg) cross-links can be directly visualized under UV light.

shape memory behavior and underlying molecular switches of traditional thermoresponsive SMPs can be investigated by differential scanning calorimetry (DSC) and especially thermomechanical dynamic mechanical analysis (DMA) studies.[6,42] However, for SMHs primarily working in aqueous solutions and displaying room-temperature shape memory behaviors, direct study of such shape memory process and supramolecular switch dynamics is difficult. Additionally, scanning electron microscopy (SEM), Fourier transform infrared spectroscopy (FT-IR), and solid-state NMR techniques, despite being able to investigate the microstructure or functional group information on cross-linked hydrogels, can only be conducted for freeze-dried hydrogel samples.

Alternatively, fluorescence-based methods have been widely used to explore dynamic processes in supramolecular/polymer science, including self-assembly and conformational changes.[43−51] Their high sensitivity allows for in situ tracking of molecular interactions even at nanomolar concentrations. More remarkably, it is possible to visualize, directly and in real time, the in situ supramolecular/polymer self-assembly process. For instance, Tang and co-workers took advantage of aggregation-induced emission fluorescent imaging to successfully show the entire gelation process of chitosan in LiOH−urea aqueous system,[49] as well as the transition processes of surfactant micelles and microemulsion droplets.[50] Yang and co-workers[51] recently reported real-time tracking of the process and dynamics of coordination-driven self-assembly through the fluorescence resonance energy transfer (FRET) technique. Li and co-workers[43] employed super-resolution fluorescence microscopy to successfully visualize the spatial distribution of organic and inorganic phases in calcium carbonate crystals, deepening the understanding of biomineralization processes and mechanisms. Enlightened by the high sensitivity and naked-eye observation of fluorescence-based methods, we herein present the first successful example of real-time in situ investigation of the dynamic metal coordination-triggered supramolecular shape memory process in SMHs.

In this study, the dynamic $Eu^{3+}$−alginate (Alg) coordination interaction was selected as the temporary switching segment and introduced into the chemically cross-linked poly(dimethylacrylamide) (PDMAA) network (permanent hard segment) to produce the PDMAA−Alg hydrogel (Figure 1a,b), based on the following three factors. First, the $Eu^{3+}$−Alg coordination interaction (Figure 1d) is quite strong but can be highly reversible in response to many external stimuli, thus ensuring effective and reproducible shape memory properties.[52] Second, $Eu^{3+}$−Alg complexes are well-known to have satisfactory photochemical stability and red-light emission intensity,[53−55] which is favorable for in situ real-time tracking of shape memory process. Finally, $Eu^{3+}$−Alg complexes and PDMAA (Figure 1c) are known as low-toxic and biocompatible materials, thus possessing a wealth of potential applications.[53]

As schematically shown in Figure 1a,b, when the non-fluorescent PDMAA−Alg hydrogel is deformed by external forces and placed into $Eu^{3+}$ ion solutions, $Eu^{3+}$ can spontaneously diffuse into the hydrogel and bind to alginate to fix the temporary shape. Due to the vivid red-light emission of Alg−$Eu^{3+}$ coordination cross-links, the dynamic metal


DOI: 10.1021/acs.jpcc.8b01689
J. Phys. Chem. C 2018, 122, 9499−9506

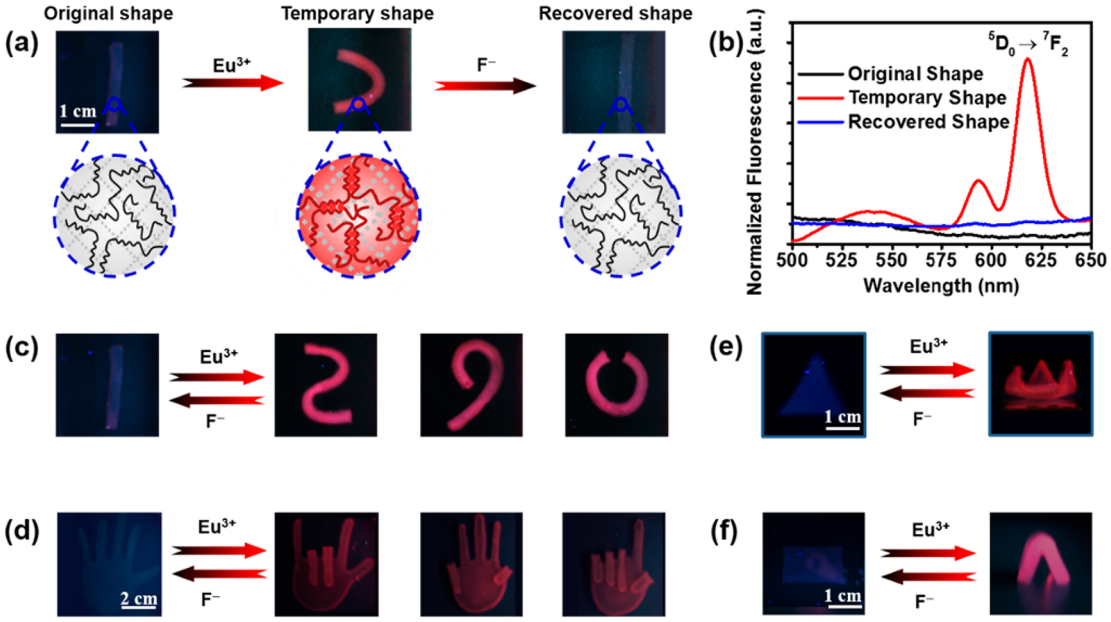


**Figure 2.** (a) Demonstration of shape memory and recovery for PDMAA−Alg-17% hydrogel. (b) Recorded fluorescence spectra of original, temporary, and recovered shapes. (c) 1D → 2D shape memory and recovery. (d) 2D → 2D shape memory and recovery. (e, f) 2D → 3D shape memory and recovery.

coordination-triggered supramolecular shape memory process could be visualized directly and quantitatively studied by fluorescence imaging methods. Importantly, in situ formation and real-time distribution of supramolecular temporary ($Eu^{3+}$−Alg) cross-links can be directly visualized under UV light. It was clearly demonstrated that the shape memory ratios of the developed SMH system are in direct proportion to the amount of Alg−$Eu^{3+}$ switching cross-links. This finding is then theoretically rationalized and modeled, which makes it possible to predict the shape memory ratios of SMHs for the first time by simple measurement of their fluorescence intensities. Furthermore, the established theoretical modeling is also successfully employed to predict shape recovery ratios of the hydrogels, and excellent agreement between the experimental and calculated results is obtained. In view of the high sensitivity and simple operation of the fluorescence approach, this method could in principle be applied to study the shape memory process of many other SMH systems.

## 2. EXPERIMENTAL SECTION

**2.1. Materials and Methods.** Potassium nitrate (99%) and ethanol (99.5%) were purchased from Shanghai Sinopharm Chemical Reagent Co. Sodium alginate (Alg, AR), bis-(acrylamide) (Bis, 98%), sodium fluoride (NaF, 99%), ammonium persulfate (APS, 99%) were purchased from Aladdin Shanghai Reagent Co. Europium(III) nitrate hydrate (99.9%, Energy Chemical Co.) and terbium(III) nitrate pentahydrate (99.9%, Aladdin Shanghai Reagent Co.) were used without further purification. *N*,*N*-Dimethylacrylamide (DMAA, 98%, J&K Scientific Ltd.) was purified by alkaline aluminum oxide column chromatography before use. Steady-state fluorescence spectra were measured under controlled conditions on a Hitachi F-4600 spectrofluorometer equipped with a xenon lamp (150 W). The transmittance spectra were conducted on a PerkinElmer Lambda 950 UV−vis−NIR spectrometer. Contrast ratio of some fluorescent images has been adjusted for clarity.

**2.2. Synthesis of PDMAA−Alg Hydrogel.** DMAA monomer and *N*,*N*′-methylenebis(acrylamide) cross-linker were first dissolved in deionized water. Then sodium alginate solution and ammonium persulfate solution were added in order and the mixture was oscillated rapidly at room temperature to give a homogeneous and viscous solution. After being transfused into the corresponding molds consisting of two glass plates and one silicone rubber template, the mixture was kept at 60 °C for 6 h to produce the highly transparent and nonfluorescent PDMAA−Alg hydrogel. PDMAA−Alg hydrogels with different Alg/(Alg + PDMAA) ratios were prepared by varying the feed ratio of Alg/DMAA by similar procedures. Hydrogel samples with various temporary shapes were prepared by manually processing the non-complexed hydrogel to a certain shape and subsequently fixing the chain conformation by $Eu^{3+}$−alginate cross-linking.[56,57]

## 3. RESULTS AND DISCUSSION

The PDMAA−Alg-*x* hydrogels, where *x* refers to the weight percentage of Alg/(Alg + PDMAA), were produced by thermally induced radical polymerization of sodium alginate, DMAA, and *N*,*N*′-methylenebis(acrylamide) cross-linker with ammonium persulfate, $(NH_4)_2S_2O_8$, as the initiator. Three hydrogel samples with different compositions (PDMAA−Alg-10%/17%/25%) were obtained by varying the Alg/DMAA feed ratio. It is known that the pendent carboxylate groups of Alg can strongly chelate with lanthanide ions such as $Eu^{3+}$, which can be employed as temporary cross-links and thus render PDMAA−Alg hydrogels with shape memory properties. As expected, both PDMAA−Alg-17% and -25% exhibit desirable shape memory performances, which are much better than that of PDMAA−Alg-10%, because higher Alg content can result in more $Eu^{3+}$−Alg cross-links. Nevertheless, it is found that PDMAA−Alg-25%, with the highest content of ionic alginate polymer, is easily swollen in aqueous solutions. Therefore, the PDMAA−Alg-17% hydrogel sample was chosen for further systematic studies.



DOI: 10.1021/acs.jpcc.8b01689
J. Phys. Chem. C 2018, 122, 9499−9506

To directly show the shape memory process of PDMAA−Alg-17%, the hydrogel samples were first prepared into straight and flat shapes. If it was doubled back by hand and immersed into aqueous $Eu^{3+}$ solution (0.3 M), the new $Eu^{3+}$-doped hybrid hydrogel could quickly hold a new two-dimensional (2D) profile within 1 min (Figure 2a). Meanwhile, the transparent PDMAA−Alg-17% hydrogel becomes slightly translucent, concomitant with the transmittance decrease from 86.6% to 80.6% at 550 nm (Figure S1). As expected, the nonfluorescent original hydrogel was found to emit vivid red fluorescence when observed under UV irradiation at 365 nm (Figure 2a). Its fluorescence spectrum displays a series of typical peaks corresponding to the intra-$4f^6$ $^5D_0 \rightarrow {}^7F_{0-4}$ transitions of $Eu^{3+}$ complexes, with a maximal emission wavelength at 618 nm ($^5D_0 \rightarrow {}^7F_2$) (Figure 2b).[52] Moreover, the original one-dimensional (1D) straight hydrogel strips could also be made to quickly hold many different 2D temporary shapes (Figure 2c). If the PDMAA−Alg-17% hydrogel was originally molded to form 2D hand-shaped triangular or quadrilateral samples, they could be programmed to perform more complex 2D → 2D (Figure 2d) or 2D → three-dimensional (3D; Figure 2e,f) shape memory behaviors at room temperature. It should be noticed that retreatment of all these temporary shapes in NaF aqueous solutions is able to regenerate the original non-fluorescent permanent shape, which can be recast into a new temporary profile (Figure S2). Taken together, these results demonstrate the powerful cycled shape memory performance of the developed PDMAA−Alg hydrogels at room temperature, which means our polymeric materials hold great potential to work as powerful smart functional materials in many fields.

For studying the shape memory process in a stepwise way, PDMAA−Alg-17% hydrogel samples were then subjected to the traditional bending test in optimized dilute $Eu(NO_3)_3$ solutions (0.01 M), because high concentrations of $Eu^{3+}$ make the shape memory process too fast. To this end, the straight hydrogel samples were first doubled back under external forces and then immersed into the $Eu^{3+}$ solutions (0.01 M) for different time intervals (Figure 3a). After release of the external deforming stress, the bending angle of the temporary shape is determined and the shape fixation ratio could be calculated according to the widely accepted method.[1] As shown in Figure 3b, the shape fixation ratio was observed to rise significantly over a period of about 10 min and soon reach a plateau, because the diffusion of $Eu^{3+}$ ions into the hydrogel strip and the resulting formation of $Eu^{3+}$−Alg temporary cross-links are typically time-dependent. Meanwhile, the fluorescence intensity was found to increase simultaneously and reach a maximum after about 10 min (Figure 3c). The possibility of $NO_3^-$ or hydrogel swelling effect was ruled out by two control experiments in which 0.01 M aqueous $Eu(NO_3)_3$ solution was replaced by aqueous solution of $KNO_3$ (0.03 M) and pure water, respectively. In these cases, no noticeable shape memory phenomenon or fluorescence increase was observed (data not shown).

Additional SEM imaging measurements and attenuated total reflectance (ATR) FT-IR spectra of the freeze-dried hydrogel samples further demonstrate the formation of metal coordination interactions between $Eu^{3+}$ and Alg polymer. As shown in Figure 4a and Figure S3, a loosely porous cross-linked network is observed for the PDMAA−Alg-17% aerogel, while much smaller pores are displayed for the $Eu^{3+}$-doped aerogel (Figure 4b), demonstrating soft matrices with quite high density of Alg−$Eu^{3+}$ coordination cross-links. The shift of the characteristic C═O stretching vibration frequency from 1600 to 1595 $cm^{-1}$ in the IR spectra (Figure 4c) reveals that the coordination interaction between $Eu^{3+}$ and the carboxyl groups of Alg indeed takes place. The appearance of the $NO_3^-$ peak at around 1300 $cm^{-1}$ further suggests that $NO_3^-$ also participates in the formation of Alg−$Eu^{3+}$ cross-links, because it is widely known that the typical IR peak of free $NO_3^-$ appears at about 1380 $cm^{-1}$ and will show a blue shift if coordinated. As expected, decomplexation of the $Eu^{3+}$−Alg temporary cross-links in aqueous NaF solutions will recover the C═O stretching vibration peak to around 1600 $cm^{-1}$ and simultaneously vanish

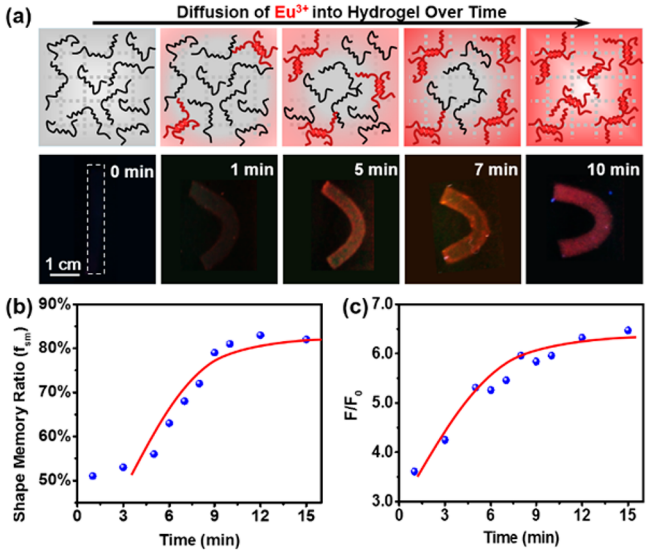


**Figure 3.** (a) Illustration and images showing the time-dependent shape memory process of the PDMAA−Alg-17% hydrogels in aqueous solutions of $Eu^{3+}$ (10 mM). The in situ formation and real-time distribution of temporary $Eu^{3+}$−Alg cross-links during shape memory process can be inferred from the fluorescence-based visual study. (b) Shape memory ratio and (c) fluorescence ratio of the arc-shaped $Eu^{3+}$-doped hybrid hydrogels as a function of time. $F_0$ and $F$ are the fluorescence intensities of the hydrogels at 618 nm before and after $Eu^{3+}$ doping, respectively.

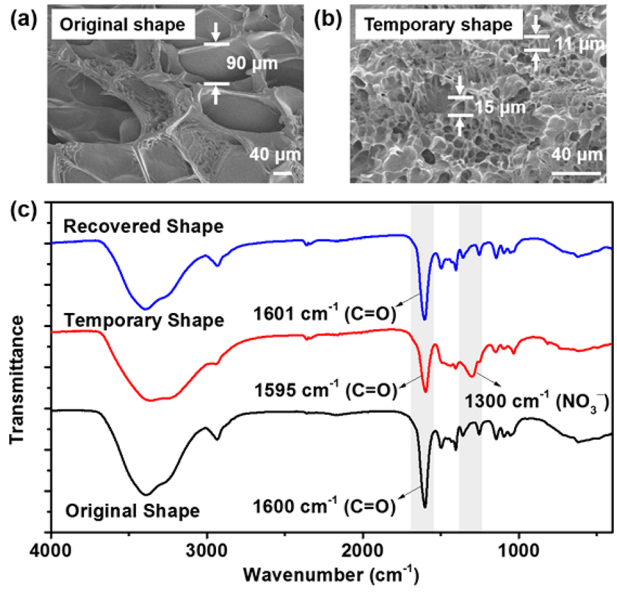


**Figure 4.** (a, b) SEM images and (c) FT-IR spectra of freeze-dried hydrogel samples of PDMAA−Alg-17% before and after $Eu^{3+}$ doping.



DOI: 10.1021/acs.jpcc.8b01689
J. Phys. Chem. C 2018, 122, 9499−9506

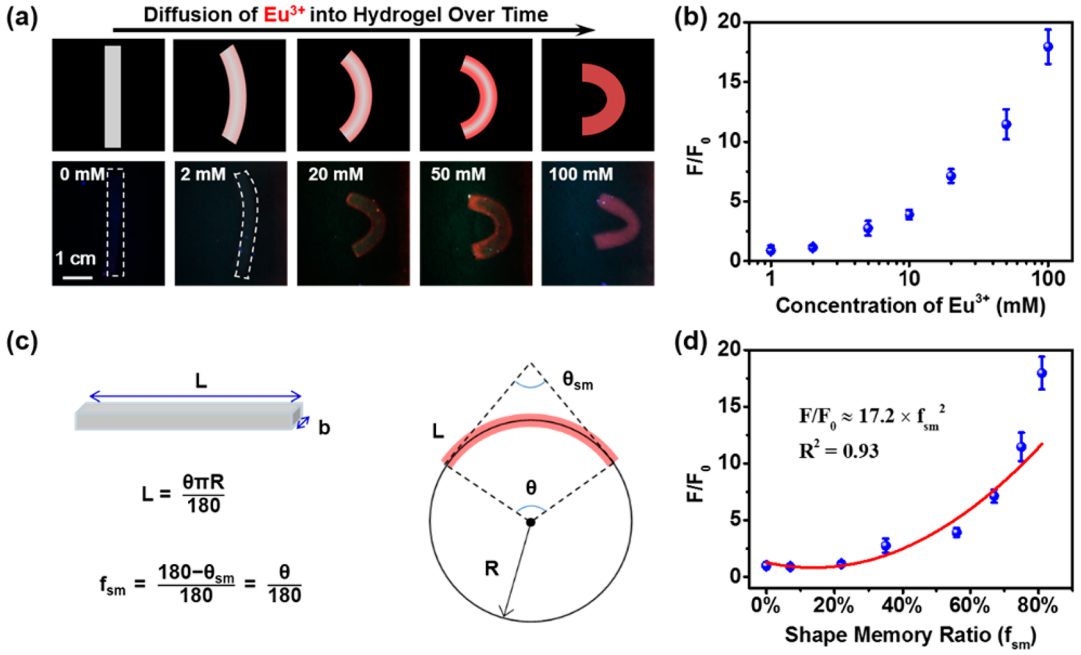


**Figure 5.** (a) Illustration and images of $Eu^{3+}$-triggered shape memory process of PDMAA−Alg-17% hydrogels. In the experiment, straight flat strips of PDMAA−Alg-17% hydrogels were first doubled back and then immersed into aqueous $Eu^{3+}$ solution of different concentrations for 1 min. These photos were taken under UV irradiation at 365 nm. (b) Fluorescence enhancement ratio ($F/F_0$) of arc-shaped $Eu^{3+}$-doped hybrid hydrogels at 618 nm as a function of $Eu^{3+}$ concentration. (c) Geometrical parameters of arc-shaped $Eu^{3+}$-doped hybrid hydrogels as well as the definition equation of shape memory ratio ($f_{sm}$). (d) Fluorescence enhancement ratio ($F/F_0$) of arc-shaped $Eu^{3+}$-doped hybrid hydrogels at 618 nm as a function of shape memory ratio ($f_{sm}$). The working curve is fitted by use of eq 5.

the coordinated $NO_3^-$ peak (Figure 4c), as well as quenching the vivid red fluorescence of the $Eu^{3+}$-doped aerogel (Figure S4). Taken together, all these studies thus provide unambiguous confirmation that $Eu^{3+}$ does indeed induce the shape memory and turn on fluorescence properties.

To obtain more insight into the supramolecular shape memory process, the relationship between fluorescence intensity and shape memory ratio ($f_{sm}$) was then investigated. For this purpose, the simplest straight to circle arc shape memory process was taken as an example and subjected to systematic studies. Accordingly, straight flat PDMAA−Alg-17% hydrogel strips were first deformed by hand and then immersed into aqueous $Eu^{3+}$ solutions of different concentrations (ranging from 0 to 100 mM) for the same period (1 min). As summarized in Figure 5a, it was found that the temporary bending curvatures rise with increasing $Eu^{3+}$ concentration, accompanied by significant enhancement of fluorescence intensity (Figure 5b and Figures S5 and S6). Interestingly, the shape memory process can be clearly visualized by the naked eye under UV light. Qualitative evaluation of the shape memory process was further addressed by developing a theoretical model that formulates the relationship between fluorescence intensity and shape memory ratio.

To theoretically account for the experimentally found bending curvatures of shape memory hydrogels, we developed a model that allows prediction of the shape memory ratio through simply measuring the fluorescence intensity of $Eu^{3+}$-doped hydrogels. The model assumes that the elastic free energy of the equilibrium temporary shape comes from Alg−$Eu^{3+}$ coordination cross-links. Solving the full elastic problem is a formidable task that moreover requires information on multiple system parameters. For simplification, we use the sum of two important elastic free energy terms, $E_{tol} = E_{ex} + E_b$, that are usually considered as parameters controlling the hydrogel stretching and bending.[58] Since our hydrogels do not undergo stretching or compression during the shape memory process, the bending free energy term corresponds to their main deformation. According to the Canham−Helfrich−Evans theory,[59−61] which relates the bending energy to bending curvature as long as the hydrogel is not too thick:

$$E_b = kLb/R^2 \tag{1}$$

where $R$ is the average hydrogel radius of curvature (Figure 5c) and $L$ and $b$ are the hydrogel length and width, respectively. In this equation, $k$ is the bending modulus, which can be typically assumed to be a constant for simplification. As displayed in Figure 5c, $L = \theta\pi R/180$, and the shape memory ratio $f_{sm} = \theta/180$ according to the widely accepted method.[1,20] Therefore, eq 1 can be transformed to

$$E_b = kb\pi^2/L \times f_{sm}^{\ 2} \tag{2}$$

The model assumes that the elastic free energy of the equilibrium temporary shape comes from Alg−$Eu^{3+}$ coordination cross-links. Therefore, $E_b$ is in direct proportion to the concentration of Alg−$Eu^{3+}$ complexes ($C_{AE}$):

$$E_b \propto C_{AE} \tag{3}$$

Additionally, the fluorescence intensity $F$ is known to be in direct proportion to the concentration of Alg−$Eu^{3+}$ complexes ($C_{AE}$) as long as their concentration is not too high (Figure S6):[62]

$$F = 2.3Y\varphi I_0 \varepsilon l C_{AE} \tag{4}$$

where $I_0$ is the intensity of excitation light, $\varphi$ is fluorescence quantum yield, $\varepsilon$ is molar absorptivity, $l$ is sample thickness, and


DOI: 10.1021/acs.jpcc.8b01689
J. Phys. Chem. C 2018, 122, 9499−9506

$Y$ is a constant determined by the sample. According to eqs 2−4, it is reasonable to conclude that

$$F/F_0 \propto f_{sm}^{\ 2} \quad (5)$$

where $F_0$ is the fluorescence intensity of free PDMAA−Alg-17% hydrogel sample.

In eq 5, a theoretical model is established that is capable of correlating fluorescence intensity with shape memory ratios ($f_{sm}$). Interestingly, we find quite good agreement between this theoretical model and our experimental data when $f_{sm}$ is less than 75% (Figure 5d), suggesting that the bending deformation energy that is accounted for in this model is the most important component and dictates the equilibrium bending curvatures. However, at higher shape memory ratio ($f_{sm}$ > 75%), there is a big deviation between experimental data and theoretically predicted results (Figure 5d). The reason for this disaggreement may come from the fact that the memorized temporary shape at high shape memory ratio (e.g., 81%; Figure 5a) is far from the standard circle arc that is assumed in this theoretical model.

In order to test the robustness of the established theoretical model, systematic studies were then conducted to compare the predicted and experimental bending values of the shape recovery process. To this end, the $Eu^{3+}$-doped hydrogels with temporary circle arc shape were immersed into fluoride solutions (0.1 M), because fluoride ion is known to bind $Eu^{3+}$ strongly and thus can destroy the temporary Alg−$Eu^{3+}$ cross-links. As can be seen in Figure 6a, the arc-shaped

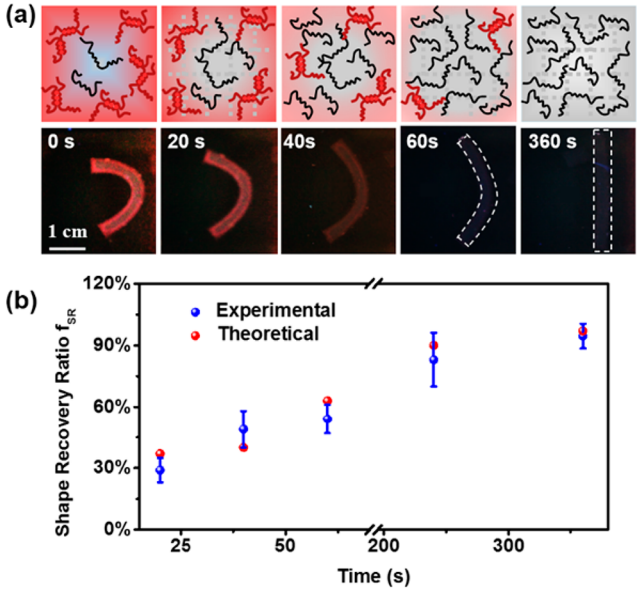


**Figure 6.** (a) Illustration and images of time-dependent shape recovery process of $Eu^{3+}$-doped hybrid hydrogels in sodium fluoride solutions (0.1 M). These photos were taken under UV irradiation at 365 nm. (b) Comparison of time-dependent experimental and theoretical shape recovery ratios ($f_{sr} = 1 - f_{sm}$) of $Eu^{3+}$-doped hybrid hydrogels. Theoretical $f_{sr}$ values were estimated by use of eq 5.

hydrogel samples do recover to the original straight shape over time, while the red-light fluorescence gradually fades at the same time. This finding is of significant interest, as it is in quite good agreement with the above-established theoretical model. Enlightened by this, we try to test the possibility that this model may be employed to theoretically predict the shape recovery ratio ($f_{sr} = 1 - f_{sm}$) of these hydrogels.[1,20] As shown in Figure 6b, we see that, upon subjecting the arc-shaped hydrogel to aqueous NaF solutions for 40 and 240 s, the shape recovery ratios are predicted to be 40% and 90%, respectively, according to the model (eq 5). These results are quite similar to the experimental values (Figure 6b), thus demonstrating that the above-mentioned theoretical model allows us to facilely predict shape recovery ratios by simply measuring the fluorescence intensity of the hydrogels without complex experimental procedures.

Besides $Eu^{3+}$, other lanthanide ions such as $Tb^{3+}$ (terbium ions) can also be used as a trigger to induce similar shape memory behavior of PDMAA−Alg-17% hydrogel but with different fluorescence color (Figures S8 and S9). As exhibited in Figure S8, $Tb^{3+}$-doped hydrogels exhibit a series of narrow fluorescence emission bands ascribed to intra-$4f_8$ $^5D_4 \rightarrow {}^7F_{6-0}$ transitions, which have a maximal emission wavelength at 544 nm ($^5D_4 \rightarrow {}^7F_5$).[54] Enlightened by the variable fluorescence color of $Eu^{3+}$- and $Tb^{3+}$-doped hydrogels, we next investigate whether it is possible to modulate the luminescence color of these shape memory hydrogels by tuning the stoichiometry of the two lanthanide chromophores (red and green). For this purpose, shape memory experiments are conducted in lanthanide solutions with different $Eu^{3+}/Tb^{3+}$ molar ratios (the total concentration is fixed at 0.3 M). As expected, treatment with different $Eu^{3+}/Tb^{3+}$ molar ratios leads to a series of circle-shaped hybrid hydrogels with a broad spectrum of emission under UV irradiation at 365 nm (Figure S9). Further fluorescence spectroscopic studies reveal that the intensity of the green band at 544 nm decreases gradually as a function of $Eu^{3+}/Tb^{3+}$ molar ratio (Figure S10). These results are of significant interest, because the straightforward fluorescence emission control of these shape memory hydrogels demonstrated here offers a simple design approach to broad-spectrum color tuning of luminescent polymeric materials.[63]

## 4. CONCLUSIONS

In conclusion, this study presents the first successful example of real-time in situ investigation of the process and dynamics of coordination-triggered supramolecular shape memory in aqueous solutions at room temperature by employing the fluorescence method. The high efficiency and sensitivity of fluorescence methods allow direct monitoring of the diffusion of $Eu^{3+}$ into the hydrogel and in situ formation of the Alg−$Eu^{3+}$ temporary cross-links, thus mapping the real-time spatial distribution of temporary supramolecular cross-links. It also enables the establishment of a theoretical model that correlates the fluorescence intensities of $Eu^{3+}$-doped PDMAA−Alg hydrogels with their SME. According to this model, both the shape memory and recovery ratios of the developed hydrogels could be facilely and accurately predicted on the basis of quantitative emission spectra results. Compared with the bending test, FT-IR, or SEM technique, the fluorescence-based approach is capable of providing much more in situ information about supramolecular chemistry switches that control the shape memory performance of SMHs. This study will thus undoubtedly deepen understanding of the metal-coordination supramolecular shape memory process and accelerate the development of new practical shape memory hydrogels in the future.



DOI: 10.1021/acs.jpcc.8b01689
J. Phys. Chem. C 2018, 122, 9499−9506

## ■ ASSOCIATED CONTENT

### Supporting Information

The Supporting Information is available free of charge on the ACS Publications website at DOI: 10.1021/acs.jpcc.8b01689.

Ten figures showing transmittance and fluorescence spectra, cycled shape memory results, SEM and UV images, relationships between $F/F_0$ and $Eu^{3+}$ concentration and between $f_{sm}$ and $Eu^{3+}$ concentration, and images of $Tb^{3+}/Eu^{3+}$ mixture-triggered SMH samples (PDF)

## ■ AUTHOR INFORMATION


### Corresponding Authors

*(J.Z.) E-mail zhangjiawei@nimte.ac.cn.
*(T.C.) E-mail tao.chen@nimte.ac.cn.

### ORCID

Jiawei Zhang: 0000-0002-3182-9239
Youju Huang: 0000-0001-5815-9784
Chih-Feng Huang: 0000-0002-8062-8708
Tao Chen: 0000-0001-9704-9545


### Notes

The authors declare no competing financial interest.

## ■ ACKNOWLEDGMENTS

We thank National Natural Science Foundation of China (21774138, 51773215, 21504100), Key Research Program of Frontier Sciences, Chinese Academy of Sciences (QYZDB-SSW-SLH036), Project of International Cooperation Foundation of Ningbo (2017D10014), Natural Science Foundation of Zhejiang (LY17B040003, LY17B040004), Youth Innovation Promotion Association of Chinese Academy of Sciences (2017337), and Open Research Fund of Key Laboratory of Marine Materials and Related Technologies (2016Z01, 2017K03).

## ■ REFERENCES


(1) Lendlein, A.; Kelch, S. Shape-Memory Polymers. *Angew. Chem., Int. Ed.* **2002**, *41*, 2034.
(2) Miyata, T.; Asami, N.; Uragami, T. A Reversibly Antigen-Responsive Hydrogel. *Nature* **1999**, *399*, 766.
(3) Osada, Y.; Matsuda, A. Shape-Memory In Hydrogels. *Nature* **1995**, *376*, 219.
(4) Xie, T. Tunable Polymer Multi-Shape Memory Effect. *Nature* **2010**, *464*, 267.
(5) Zhao, Q.; Zou, W. K.; Luo, Y. W.; Xie, T. Shape Memory Polymer Network With Thermally Distinct Elasticity And Plasticity. *Sci. Adv.* **2016**, *2*, No. e1501297.
(6) Zhao, Q.; Qi, H. J.; Xie, T. Recent Progress In Shape Memory Polymer: New Behavior, Enabling Materials, And Mechanistic Understanding. *Prog. Polym. Sci.* **2015**, *49−50*, 79.
(7) Habault, D.; Zhang, H.; Zhao, Y. Light-Triggered Self-Healing And Shape-Memory Polymers. *Chem. Soc. Rev.* **2013**, *42*, 7244.
(8) Li, X.; Serpe, M. J. Understanding The Shape Memory Behavior Of Self-Bending Materials And Their Use As Sensors. *Adv. Funct. Mater.* **2016**, *26*, 3282.
(9) Zhang, Q. M.; Serpe, M. J. Stimuli-Responsive Polymers For Actuation. *ChemPhysChem* **2017**, *18*, 1451.
(10) Leng, J.; Lan, X.; Liu, Y.; Du, S. Stimuli-Responsive Polymers For Actuation. *Prog. Mater. Sci.* **2011**, *56*, 1077.
(11) Samra, B. K.; Galaev, I. Y.; Mattiasson, B. Thermosensitive, Reversibly Cross-Linking Gels With A Shape "Memory". *Angew. Chem., Int. Ed.* **2000**, *39*, 2364.
(12) Liu, C.; Qin, H.; Mather, P. T. Review Of Progress In Shape-Memory Polymers. *J. Mater. Chem.* **2007**, *17*, 1543.
(13) Small, W., IV; Singhal, P.; Wilson, T. S.; Maitland, D. J. Biomedical Applications Of Thermally Activated Shape Memory Polymers. *J. Mater. Chem.* **2010**, *20*, 3356.
(14) Lewis, C. L.; Dell, E. M. A Review Of Shape Memory Polymers Bearing Reversible Binding Groups. *J. Polym. Sci., Part B: Polym. Phys.* **2016**, *54*, 1340.
(15) Wang, K. J.; Strandman, S.; Zhu, X. X. A Mini Review: Shape Memory Polymers For Biomedical Applications. *Front. Chem. Sci. Eng.* **2017**, *11*, 143.
(16) Gautrot, J. E.; Zhu, X. X. Shape Memory Polymers Based On Naturally-Occurring Bile Acids. *Macromolecules* **2009**, *42*, 7324.
(17) Shao, Y.; Lavigueur, C.; Zhu, X. X. Multishape Memory Effect Of Norbornene-Based Copolymers With Cholic Acid Pendant Groups. *Macromolecules* **2012**, *45*, 1924.
(18) Wang, K. J.; Jia, Y. G.; Zhu, X. X. Two-Way Reversible Shape Memory Polymers Made Of Cross-Linked Cocrystallizable Random Copolymers With Tunable Actuation Temperatures. *Macromolecules* **2017**, *50*, 8570.
(19) Lu, W.; Le, X. X.; Zhang, J. W.; Huang, Y. J.; Chen, T. Supramolecular Shape Memory Hydrogels: A New Bridge Between Stimuli-Responsive Polymers And Supramolecular Chemistry. *Chem. Soc. Rev.* **2017**, *46*, 1284.
(20) Le, X. X.; Lu, W.; Zheng, J.; Tong, D. Y.; Zhao, N.; Ma, C. X.; Xiao, H.; Zhang, J. W.; Huang, Y. J.; Chen, T. Stretchable Supramolecular Hydrogels With Triple Shape Memory Effect. *Chem. Sci.* **2016**, *7*, 6715.
(21) Xiao, H.; Lu, W.; Le, X.; Ma, C.; Li, Z.; Zheng, J.; Zhang, J.; Huang, Y.; Chen, T. A Multi-Responsive Hydrogel With A Triple Shape Memory Effect Based On Reversible Switches. *Chem. Commun.* **2016**, *52*, 13292.
(22) Meng, H.; Xiao, P.; Gu, J. C.; Wen, X. F.; Xu, J.; Zhao, C. Z.; Zhang, J. W.; Chen, T. Self-Healable Macro-/Microscopic Shape Memory Hydrogels Based On Supramolecular Interactions. *Chem. Commun.* **2014**, *50*, 12277.
(23) Lowenberg, C.; Balk, M.; Wischke, C.; Behl, M.; Lendlein, A. Shape-Memory Hydrogels: Evolution Of Structural Principles To Enable Shape Switching Of Hydrophilic Polymer Networks. *Acc. Chem. Res.* **2017**, *50*, 723.
(24) Chan, B. Q.; Low, Z. W.; Heng, S. J.; Chan, S. Y.; Owh, C.; Loh, X. J. Recent Advances In Shape Memory Soft Materials For Biomedical Applications. *ACS Appl. Mater. Interfaces* **2016**, *8*, 10070.
(25) Guo, W.; Lu, C. H.; Orbach, R.; Wang, F.; Qi, X. J.; Cecconello, A.; Seliktar, D.; Willner, I. Ph-Stimulated Dna Hydrogels Exhibiting Shape-Memory Properties. *Adv. Mater.* **2015**, *27*, 73.
(26) Hu, Y.; Guo, W.; Kahn, J. S.; Aleman-Garcia, M. A.; Willner, I. A Shape-Memory Dna-Based Hydrogel Exhibiting Two Internal Memories. *Angew. Chem., Int. Ed.* **2016**, *55*, 4210.
(27) Miyamae, K.; Nakahata, M.; Takashima, Y.; Harada, A. Self-Healing, Expansion-Contraction, And Shape-Memory Properties Of A Preorganized Supramolecular Hydrogel Through Host-Guest Interactions. *Angew. Chem., Int. Ed.* **2015**, *54*, 8984.
(28) Jiang, Z. C.; Xiao, Y. Y.; Kang, Y.; Pan, M.; Li, B. J.; Zhang, S. Shape Memory Polymers Based On Supramolecular Interactions. *ACS Appl. Mater. Interfaces* **2017**, *9*, 20276.
(29) Xiao, Y. Y.; Gong, X. L.; Kang, Y.; Jiang, Z. C.; Zhang, S.; Li, B. J. Light-, Ph- And Thermal-Responsive Hydrogels With The Triple-Shape Memory Effect. *Chem. Commun.* **2016**, *52*, 10609.
(30) Harris, R. D.; Auletta, J. T.; Motlagh, S. A. M.; Lawless, M. J.; Perri, N. M.; Saxena, S.; Weiland, L. M.; Waldeck, D. H.; Clark, W. W.; Meyer, T. Y. Chemical And Electrochemical Manipulation Of Mechanical Properties In Stimuli-Responsive Copper-Cross-Linked Hydrogels. *ACS Macro Lett.* **2013**, *2*, 1095.
(31) Feng, W.; Zhou, W. F.; Dai, Z. H.; Yasin, A.; Yang, H. Y. Tough Polypseudorotaxane Supramolecular Hydrogels With Dual-Responsive Shape Memory Properties. *J. Mater. Chem. B* **2016**, *4*, 1924.
(32) Ren, Z. Q.; Zhang, Y. Y.; Li, Y. M.; Xu, B.; Liu, W. G. Hydrogen Bonded And Ionically Crosslinked High Strength Hydrogels




DOI: 10.1021/acs.jpcc.8b01689
J. Phys. Chem. C 2018, 122, 9499−9506

Exhibiting Ca2+-Triggered Shape Memory Properties And Volume Shrinkage For Cell Detachment. *J. Mater. Chem. B* **2015**, *3*, 6347.
(33) Huang, J. H.; Zhao, L.; Wang, T.; Sun, W. X.; Tong, Z. Nir-Triggered Rapid Shape Memory Pam-Go-Gelatin Hydrogels With High Mechanical Strength. *ACS Appl. Mater. Interfaces* **2016**, *8*, 12384.
(34) Zhang, Y. Y.; Li, Y. M.; Liu, W. G. Dipole-Dipole And H-Bonding Interactions Significantly Enhance The Multifaceted Mechanical Properties Of Thermoresponsive Shape Memory Hydrogels. *Adv. Funct. Mater.* **2015**, *25*, 471.
(35) Liao, J. X.; Huang, J. H.; Wang, T.; Sun, W. X.; Tong, Z. Rapid Shape Memory And Ph-Modulated Spontaneous Actuation Of Dopamine Containing Hydrogels. *Chin. J. Polym. Sci.* **2017**, *35*, 1297.
(36) Wang, W.; Zhang, Y. Y.; Liu, W. G. Bioinspired Fabrication Of High Strength Hydrogels From Non-Covalent Interactions. *Prog. Polym. Sci.* **2017**, *71*, 1.
(37) Kurt, B.; Gulyuz, U.; Demir, D. D.; Okay, O. High-Strength Semi-Crystalline Hydrogels With Self-Healing And Shape Memory Functions. *Eur. Polym. J.* **2016**, *81*, 12.
(38) Bilici, C.; Can, V.; Nöchel, U.; Behl, M.; Lendlein, A.; Okay, O. Melt-Processable Shape-Memory Hydrogels With Self-Healing Ability Of High Mechanical Strength. *Macromolecules* **2016**, *49*, 7442.
(39) Yang, L.; Tan, X.; Wang, Z.; Zhang, X. Supramolecular Polymers: Historical Development, Preparation, Characterization, And Functions. *Chem. Rev.* **2015**, *115*, 7196.
(40) Yu, G.; Jie, K.; Huang, F. Supramolecular Amphiphiles Based On Host-Guest Molecular Recognition Motifs. *Chem. Rev.* **2015**, *115*, 7240.
(41) Das, A.; Theato, P. Activated Ester Containing Polymers: Opportunities And Challenges For The Design Of Functional Macromolecules. *Chem. Rev.* **2016**, *116*, 1434.
(42) Hornat, C. C.; Yang, Y.; Urban, M. W. Quantitative Predictions Of Shape-Memory Effects In Polymers. *Adv. Mater.* **2017**, *29*, No. 1603334.
(43) Fu, M.; Wang, A.; Zhang, X.; Dai, L.; Li, J. Direct Observation Of The Distribution Of Gelatin In Calcium Carbonate Crystals By Super-Resolution Fluorescence Microscopy. *Angew. Chem., Int. Ed.* **2016**, *55*, 908.
(44) Valkenier, H.; Lopez Mora, N.; Kros, A.; Davis, A. P. Visualization And Quantification Of Transmembrane Ion Transport Into Giant Unilamellar Vesicles. *Angew. Chem., Int. Ed.* **2015**, *54*, 2137.
(45) Vukotic, V. N.; Zhu, K.; Baggi, G.; Loeb, S. J. Optical Distinction Between ″Slow″ And ″Fast″ Translational Motion In Degenerate Molecular Shuttles. *Angew. Chem., Int. Ed.* **2017**, *56*, 6136.
(46) Ye, X.; Liu, Y.; Lv, Y.; Liu, G.; Zheng, X.; Han, Q.; Jackson, K. A.; Tao, X. In Situ Microscopic Observation Of The Crystallization Process Of Molecular Microparticles By Fluorescence Switching. *Angew. Chem., Int. Ed.* **2015**, *54*, 7976.
(47) Bao, C.; Pahler, G.; Geil, B.; Janshoff, A. Optical Fusion Assay Based On Membrane-Coated Spheres In A 2d Assembly. *J. Am. Chem. Soc.* **2013**, *135*, 12176.
(48) Gong, B.; Choi, B. K.; Kim, J. Y.; Shetty, D.; Ko, Y. H.; Selvapalam, N.; Lee, N. K.; Kim, K. High Affinity Host-Guest Fret Pair For Single-Vesicle Content-Mixing Assay: Observation Of Flickering Fusion Events. *J. Am. Chem. Soc.* **2015**, *137*, 8908.
(49) Wang, Z. K.; Nie, J. Y.; Qin, W.; Hu, Q. L.; Tang, B. Z. Gelation Process Visualized By Aggregation-Induced Emission Fluorogens. *Nat. Commun.* **2016**, *7*, 12033.
(50) Guan, W.; Zhou, W.; Lu, C.; Tang, B. Z. Synthesis And Design Of Aggregation-Induced Emission Surfactants: Direct Observation Of Micelle Transitions And Microemulsion Droplets. *Angew. Chem., Int. Ed.* **2015**, *54*, 15160.
(51) Huang, C. B.; Xu, L.; Zhu, J. L.; Wang, Y. X.; Sun, B.; Li, X.; Yang, H. B. Real-Time Monitoring The Dynamics Of Coordination-Driven Self-Assembly By Fluorescence-Resonance Energy Transfer. *J. Am. Chem. Soc.* **2017**, *139*, 9459.
(52) Li, B.; Wen, H.-M.; Cui, Y.; Qian, G.; Chen, B. Multifunctional Lanthanide Coordination Polymers. *Prog. Polym. Sci.* **2015**, *48*, 40.
(53) Liu, F. Y.; Carlos, L. D.; Ferreira, R. A. S.; Rocha, J.; Gaudino, M. C.; Robitzer, M.; Quignard, F. Photoluminescent Porous Alginate Hybrid Materials Containing Lanthanide Ions. *Biomacromolecules* **2008**, *9*, 1945.
(54) Ma, Q.; Wang, Q. Lanthanide Induced Formation Of Novel Luminescent Alginate Hydrogels And Detection Features. *Carbohydr. Polym.* **2015**, *133*, 19.
(55) Wang, M. X.; Yang, C. H.; Liu, Z. Q.; Zhou, J.; Xu, F.; Suo, Z.; Yang, J. H.; Chen, Y. M. Tough Photoluminescent Hydrogels Doped With Lanthanide. *Macromol. Rapid Commun.* **2015**, *36*, 465.
(56) Choi, S.; Kim, J. Designed Fabrication Of Super-Stiff, Anisotropic Hybrid Hydrogels Via Linear Remodeling Of Polymer Networks And Subsequent Crosslinking. *J. Mater. Chem. B* **2015**, *3*, 1479.
(57) Lin, P.; Zhang, T.; Wang, X.; Yu, B.; Zhou, F. Freezing Molecular Orientation Under Stretch For High Mechanical Strength But Anisotropic Hydrogels. *Small* **2016**, *12*, 4386.
(58) Hu, Y.; Kahn, J. S.; Guo, W.; Huang, F.; Fadeev, M.; Harries, D.; Willner, I. Reversible Modulation Of Dna-Based Hydrogel Shapes By Internal Stress Interactions. *J. Am. Chem. Soc.* **2016**, *138*, 16112.
(59) Canham, P. B. Minimum Energy Of Bending As A Possible Explanation Of Biconcave Shape Of Human Red Blood Cell. *J. Theor. Biol.* **1970**, *26*, 61.
(60) Helfrich, W. Z. Elastic Properties Of Lipid Bilayers: Theory And Possible Experiments. *Z. Naturforsch., C: J. Biosci.* **1973**, *28*, 693.
(61) Evans, E. A. Bending Resistance And Chemically-Induced Moments In Membrane Bilayers. *Biophys. J.* **1974**, *14*, 923.
(62) Fan, M. G.; Yao, J. N.; Tong, Z. H. *Molecular Photochemistry and Optical Functional Materials Science*; Science Press: Beijing, 2009.
(63) Chen, P.; Li, Q.; Grindy, S.; Holten-Andersen, N. White-Light-Emitting Lanthanide Metalloge's With Tunable Luminescence And Reversible Stimuli-Responsive Properties. *J. Am. Chem. Soc.* **2015**, *137*, 11590.


DOI: 10.1021/acs.jpcc.8b01689
*J. Phys. Chem. C* 2018, 122, 9499−9506